


CYT-Rx20 inhibits ovarian cancer cells in vitro and in vivo through oxidative stress-induced DNA damage and cell apoptosis

Yen-Yun Wang¹  · Yuk-Kwan Chen^{2,3,4} · Stephen Chu-Sung Hu^{5,6} · Ya-Ling Hsu¹ · Chun-Hao Tsai⁷ · Tsung-Chen Chi¹ · Wan-Ling Huang¹ · Pei-Wen Hsieh^{8,9,10} · Shyng-Shiou F. Yuan^{1,7,11,12}

Received: 21 December 2016 / Accepted: 2 May 2017 / Published online: 12 May 2017
© Springer-Verlag Berlin Heidelberg 2017

Abstract

Purpose The β -nitrostyrene family has been previously reported to possess anticancer property. However, the biological effects of β -nitrostyrenes on ovarian cancer and the underlying mechanisms involved remain unclear. In the present study, we synthesized a β -nitrostyrene derivative, CYT-Rx20 (3'-hydroxy-4'-methoxy- β -methyl- β -nitrostyrene), and investigated its anticancer effects and the putative pathways of action in ovarian cancer.

Methods The effects of CYT-Rx20 were analyzed using cell viability assay, reactive oxygen species (ROS) generation assay, FACS analysis, annexin V staining, immunostaining, comet assay, immunoblotting, soft agar

assay, migration assay, nude mice xenograft study and immunohistochemistry.

Results CYT-Rx20 induced cytotoxicity in ovarian cancer cells by promoting cell apoptosis via ROS generation and DNA damage. CYT-Rx20-induced cell apoptosis, ROS generation and DNA damage were reversed by thiol antioxidants. In addition, CYT-Rx20 inhibited ovarian cancer cell migration by regulating the expression of epithelial to mesenchymal transition (EMT) markers. In nude mice, CYT-Rx20 inhibited ovarian tumor growth accompanied by increased expression of DNA damage marker γ H2AX and decreased expression of EMT marker Vimentin.

Conclusions CYT-Rx20 inhibits ovarian cancer cells in vitro and in vivo, and has the potential to be further developed into an anti-ovarian cancer drug clinically.

Electronic supplementary material The online version of this article (doi:10.1007/s00280-017-3330-9) contains supplementary material, which is available to authorized users.

✉ Shyng-Shiou F. Yuan
yuanssf@kmu.edu.tw

- ¹ Department of Medical Research, Kaohsiung Medical University Hospital, Kaohsiung Medical University, Kaohsiung, Taiwan
- ² Division of Oral Pathology and Maxillofacial Radiology, Kaohsiung Medical University Hospital, Kaohsiung, Taiwan
- ³ School of Dentistry, College of Dental Medicine, Kaohsiung Medical University, Kaohsiung, Taiwan
- ⁴ Oral and Maxillofacial Imaging Center, College of Dental Medicine, Kaohsiung Medical University, Kaohsiung, Taiwan
- ⁵ Department of Dermatology, College of Medicine, Kaohsiung Medical University, Kaohsiung, Taiwan
- ⁶ Department of Dermatology, Kaohsiung Medical University Hospital, Kaohsiung Medical University, Kaohsiung, Taiwan

Keywords β -Nitrostyrene · ROS · Apoptosis · Migration · Ovarian cancer

- ⁷ Graduate Institute of Medicine, College of Medicine, Kaohsiung Medical University, Kaohsiung, Taiwan
- ⁸ Graduate Institute of Natural Products, School of Traditional Chinese Medicine, Chang Gung University, Taoyuan, Taiwan
- ⁹ Graduate Institute of Biomedical Sciences, College of Medicine, Chang Gung University, Taoyuan, Taiwan
- ¹⁰ Department of Anesthesiology, Chang Gung Memorial Hospital, Taoyuan, Taiwan
- ¹¹ Translational Research Center, Kaohsiung Medical University Hospital, Kaohsiung Medical University, No.100, Tzyou 1st Road, 807, Kaohsiung, Taiwan
- ¹² Department of Obstetrics and Gynecology, Kaohsiung Medical University Hospital, Kaohsiung Medical University, Kaohsiung, Taiwan

Introduction

Ovarian cancer is the third most common lethal gynecologic malignancy worldwide [1]. Over 90% of ovarian cancer deaths are caused by drug resistance and tumor metastasis [2]. Most patients undergo cytoreductive surgery and receive a combination of paclitaxel and platinum-based chemotherapy [3]. The overall 5-year survival rate in advanced ovarian cancer patients is ~40% [2, 3]. This highlights the need for continuous efforts to develop novel effective chemotherapeutic agents with low toxicity for ovarian cancer patients.

The β -nitrostyrene-derived compounds have been shown to inhibit protein tyrosine phosphatases [4] and exert diverse biological functions including anti-platelet and anticancer activities, including induction of breast cancer cell death [5–7]. 3, 4-Methylenedioxy- β -nitrostyrene exhibits anti-inflammatory effects through inactivation of NLRP3 inflammasome [8]. Regarding anticancer activities, 3,4-methylenedioxy- β -nitrostyrene reduces β 1 integrin activation and clustering, resulting in decreased adhesion of triple-negative breast cancer cell lines [5]. In addition, β -nitrostyrene inhibits gastric cancer cell proliferation and immune responses of macrophages [9], and its derivatives suppress the TNF α /NF κ B signaling pathway in a retinoid X receptor α (RXR α)-dependent manner to induce apoptosis in breast cancer cells [10].

In our previous work, we showed that CYT-Rx20 induced apoptosis in breast cancer cells through reactive oxygen species-mediated MEK-ERK signaling [11]. However, to our knowledge, the chemotherapeutic effect of CYT-Rx20 on ovarian cancer has not been investigated. Herein, we explored the potential anticancer activities of CYT-Rx20 on ovarian cancer and addressed the underlying mechanisms.

Materials and methods

Reagents

CYT-Rx20 was synthesized as previously described [12]. Dulbecco's modified Eagle medium (DMEM) and DCFDA were obtained from Invitrogen (Carlsbad, CA, USA). Annexin V/PI apoptosis detection kit was obtained from BD Biosciences (Franklin Lakes, NJ, USA). Fetal bovine serum, penicillin, streptomycin, and amphotericin B were obtained from Biological Industries (Beit Haemek, Israel). 4,6-Diamidino-2-phenylindole (DAPI), propidium iodide, and *N*-acetyl-L-cysteine (NAC) were obtained from Sigma-Aldrich (St Louis, MO, USA). Antibodies used in this study included PARP (#9542, Cell Signaling Tech.,

Danvers, MA, USA), caspase-3 (Clone 31A1067, #NB100-56708, Novus Biologicals, Littleton, CO, USA), caspase-9 (#9508, Cell Signaling Tech., Danvers, MA, USA), Histone H2AX (Clone 3F2, #GTX80694; Genetex, Irvine, CA), E-cadherin (Clone HECD-1, #ab1416, Abcam PLC, Cambridge, UK), Vimentin (#GTx100619, Genetex, Irvine, CA), Twist (#orb13736, Biorbyt, Cambridge, UK), and β -actin (#GTX110564, Genetex, Irvine, CA). Other reagents employed in the current study were indicated separately wherever suitable.

Cell culture

Three human ovarian cancer cell lines (MDAH 2774, PA-1, and SKOV3) were included in this study. Cells were grown in DMEM supplemented with 10% fetal bovine serum, 100 U/ml penicillin, 100 μ g/ml streptomycin, and 2.5 μ g/ml amphotericin B at 37 °C in a 5% CO₂ incubator.

XTT cell viability assay

Cells from three human ovarian cancer cell lines (MDAH 2774, PA-1, and SKOV3) were seeded at a density of 4×10^3 cells/well in 96-well plates and allowed to attach overnight. After treatment with CYT-Rx20 or cisplatin (CDDP) at various concentrations for 24 h, cell viability was determined by XTT colorimetric assay. 2,3-Bis(2-methoxy-4-nitro-5-sulfophenyl)-2H-tetrazolium-5-carboxanilide (Sigma-Aldrich, USA) was added into wells with PMS (*N*-methyl dibenzopyrazine methyl sulfate, Sigma-Aldrich, USA). Absorbance was measured by a spectrophotometer at 475 nm with a reference wavelength at 660 nm. Relative number of viable cells as compared to the number of cells without drug treatment was expressed as percent cell viability using the following formula: cell viability (%) = A_{475} of treated cells/ A_{475} of untreated cells.

Flow cytometry

Intracellular ROS content of human ovarian cancer cells was measured using H₂DCFDA fluorescent dye and determined by flow cytometry with the detailed procedures described in a previous report [13].

Neutral comet assay for detection of DNA double-strand breaks (DSBs)

DSBs were determined by neutral comet single-cell gel electrophoresis according to our previous report [14].

Cells from human ovarian cancer cell lines (MDAH 2774, PA-1, and SKOV3), after CYT-Rx20 treatment with the indicated concentrations for 24 h, were combined with 1% low melting point agarose at a ratio of 1:10 (v/v). 75 μ l of the mixture was immediately pipetted onto Comet Slide (Trevigen; Gaithersburg, MD, USA) at 4 °C and kept in the dark for 10 min. The slides were then immersed in prepared cold lysis solution (Trevigen) for 60 min. Subsequently, the slides were drained and placed in a horizontal gel electrophoresis apparatus containing freshly prepared neutral buffer (90 mM Tris–HCl, 90 mM boric acid, and 2 mM EDTA, pH 8.0) at 20 V for 30 min, and stained with 2.5 μ g/ml PI (Sigma-Aldrich) for 15 min. The mean tail moment was analyzed by CometScore software (TriTek; Sumerduck, VA, USA).

Immunostaining of γ H2AX foci

Cells were seeded at 1×10^4 cells/well in eight-well chamber slides (Lab-Tek II) and incubated for 24 h before treatment. After CYT-Rx20 treatment alone or pre-treatment with NAC followed by CYT-Rx20, the cells were fixed immediately in 4% paraformaldehyde. Antibody incubations were performed at room temperature and cells were counterstained with DAPI. Images were captured with a Nikon Eclipse Ti-S inverted research microscope (Japan) with excitation at 465–495 nm and 515–555 nm emission filter.

Immunoblotting analysis

The levels of caspase-associated proteins (caspase-3 and caspase-9), cleaved PARP, γ H2AX, and epithelial–mesenchymal transition (EMT) markers, including E-cadherin, Vimentin, and Twist were analyzed by immunoblotting after treatment of cells with CYT-Rx20 for 24 h. Equal amounts of proteins were resolved by SDS-PAGE and transferred to a polyvinyl difluoride (PVDF) membrane. PVDF membrane was blocked with 5% skim milk at room temperature for 1 h, and then incubated with antibodies against caspase-3, caspase-9, cleaved PARP, γ H2AX, E-cadherin, Vimentin, or Twist at 4 °C overnight. After washing with $1 \times$ TBST (Tris-buffered saline with Tween20), the membrane was incubated with horseradish peroxidase-conjugated secondary antibodies (1:5000, Thermo Scientific) at room temperature for 1 h. The immunoblots were visualized using enhanced chemiluminescence (ECL, Perkin Elmer, USA). Finally, the images were captured by ChemiDoc XRS + System (BIO-RAD, USA) and quantified by the Image LabTM software (BIO-RAD, USA).

Annexin V/PI analysis

Cell apoptosis was assessed by labeling cells with annexin V-FITC and PI. After treatment with CYT-Rx20, the cells were collected and washed twice with cold PBS and then adjusted to 5×10^5 cells/500 μ l in binding buffer containing annexin V-FITC (1 μ g/ml) and PI before analysis by flow cytometry (FC 500 MCL, Beckman Coulter, Brea, CA, USA).

Anoikis assay

Cells from three human ovarian cancer cell lines (MDAH 2774, PA-1, and SKOV3) were treated with CYT-Rx20 for 24 h. Cells (1×10^4) were resuspended in DMEM with 10% FBS onto ultra-low attachment 24-well plates (Corning, NY, USA). After 48-h incubation at 37 °C, cell viability was determined by staining with trypan blue (Sigma) in PBS (ratio of 1:1) before examination under a Nikon Eclipse TS100 microscope (Tokyo, Japan).

Cell migration assay

Cell migration was determined by a modified Boyden chamber assay. Cells (5×10^4 cells/well) suspended in 2% FBS medium were placed into the upper chamber of 8- μ m pore size transwells (24-well, Corning Life Sciences, Corning, NY), and medium with 10% FBS was added to the lower chamber. After 24-h incubation, the unigrated cells were removed from the upper surface of the transwell membrane, whereas the cells that have migrated to the underside of the membrane were stained with 0.5 g/l of crystal violet (Sigma-Aldrich, St Louis, MO, USA). The cell migration was determined by counting the number of migrated cells under a microscope at 100 \times magnification. Four visual fields were chosen randomly and the average number of migrated cells in the four fields was calculated for each group.

Anchorage-independent soft agar assay

Cells from three human ovarian cancer cell lines (MDAH 2774, PA-1, and SKOV3) were embedded in 0.25% agarose at a density of 1000 cells/well in 48-well plates, followed by treatment with CYT-Rx20 for 24 h. Cells were grown for 30 days and then stained with 0.5% crystal violet. Cell culture medium was changed every 2–3 days during the incubation period.

Ex vivo tumor xenograft study

The animal studies were approved by the Institutional Animal Care and Use Committee (IACUC No. 102009)

of Kaohsiung Medical University, Taiwan. Animal experiments were approved by the Laboratory Animal Ethics Committee of Kaohsiung Medical University and were conducted in accordance with the animal research: reporting in vivo experiments (ARRIVE) guidelines. Six-week-old female immune-deficient BALB/cAnN.Cg-*Foxn1*^{nu}/CrINarl mice from National Laboratory Animal Center of Taiwan were subcutaneously injected with 3×10^6 MDAH 2774 cells into both flanks. When the tumors grew to visible size (approximately an average diameter of 3 mm), the mice were intraperitoneally injected three times a week with DMSO-dissolved CYT-Rx20 and then diluted with 100 μ l of normal saline (0.1% DMSO) at 10.0 μ g/g body weight, whereas the control mice were intraperitoneally injected with 0.1% DMSO in normal saline alone. Tumor volumes were calculated using the formula $(\text{width}^2 \times \text{length})/2$. Tumor weights were measured when the mice were killed at the end of the experimental period.

Immunohistochemistry and hematoxylin and eosin staining

Immunohistochemical staining for γ H2AX and Vimentin were performed using the fully automated Bond-Max system and according to the manufacturer's instructions (Leica Microsystems, Wetzlar, Germany). For quantification, the staining of γ H2AX and Vimentin was evaluated. The percentage of positive-stained tumor cells was determined semiquantitatively by assessing the tumor section, and each sample was then assigned to one of the following categories: 0 (0–4%), 1 (5–24%), 2 (25–49%), 3 (50–74%), or 4 (75–100%) [15]. Additionally, the intensity of immunostaining was determined as 0 (negative), 1 (weak), 2 (moderate), or 3 (strong) for antigens with nuclear localization. The total score is designated as the percentage of positively stained cells multiplied by the weighted intensity of staining for each sample. Besides, the tissues from various organs of mice were stained with hematoxylin and eosin.

Statistical analysis

Quantitative data were presented as mean \pm SD or mean \pm SEM from three independent experiments. Differences between treatment groups were calculated by one-way analysis of variance (ANOVA) and post hoc Tukey's test for multiple comparisons. A *P* value less than 0.05 was considered statistically significant.

Results

The effect of CYT-Rx20 on ovarian cancer cell viability

Seven β -nitrostyrene derivatives (Fig. 1a; Suppl. Figure 1) were synthesized according to our previous report [7], and their cytotoxic effects on human ovarian cancer cells were analyzed by XTT assay (Table 1). Notably, CYT-Rx20 (Fig. 1a) exhibited more potent cytotoxic effect against ovarian cancer cells than other compounds (Table 1). To study the anti-ovarian cancer activity of CYT-Rx20, the cytotoxicity of CYT-Rx20 on human ovarian cell lines MDAH 2774, PA-1, and SKOV3 was analyzed (Table 2). The concentrations of half inhibition (IC_{50}) of CYT-Rx20 on these three ovarian cancer cell lines were 2.41 ± 0.16 , 2.35 ± 0.16 , and 2.48 ± 0.08 μ g/ml, respectively. In addition, CYT-Rx20 had more potent cytotoxic activity than cisplatin on two ovarian cancer cell lines (Table 2).

Involvement of ROS-mediated pathways in CYT-Rx20-induced DNA double-strand breaks in ovarian cancer cells

Reactive oxygen species (ROS) are crucial for signal transduction in response to environmental stress [16–18]. Intracellular ROS levels in ovarian cancer cells, determined by flow cytometry using the H2DCFDA fluorescent dye, showed a dose-dependent increase after CYT-Rx20 treatment for 1 h (Suppl. Figure 2a).

H2AX is a key factor in the repair process of damaged DNA [19]. When endogenous or exogenous DNA damage causes double-stranded breaks (DSBs), it is always followed by the phosphorylation of histone H2AX [19]. In this study, the DNA double-strand breaks caused by CYT-Rx20 were further analyzed by neutral comet assay (Suppl. Figure 2b), and the result revealed that CYT-Rx20 treatment led to an increase in DNA double-strand breaks. The immunocytochemistry result also showed a dose-dependent increase of γ H2AX formation in ovarian cancer cells after CYT-Rx20 treatment for 24 h in a dose-dependent manner (Suppl. Figure 2c). Notably, the CYT-Rx20-induced ROS production was reversed by co-treatment with NAC, a thiol antioxidant (Fig. 1b). The involvement of ROS in CYT-Rx20-reduced DNA damage was further determined, and the results showed that NAC significantly suppressed CYT-Rx20-induced DNA double-strand breaks and γ H2AX formation in ovarian cancer cells (Fig. 1c, d).

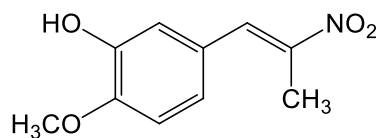
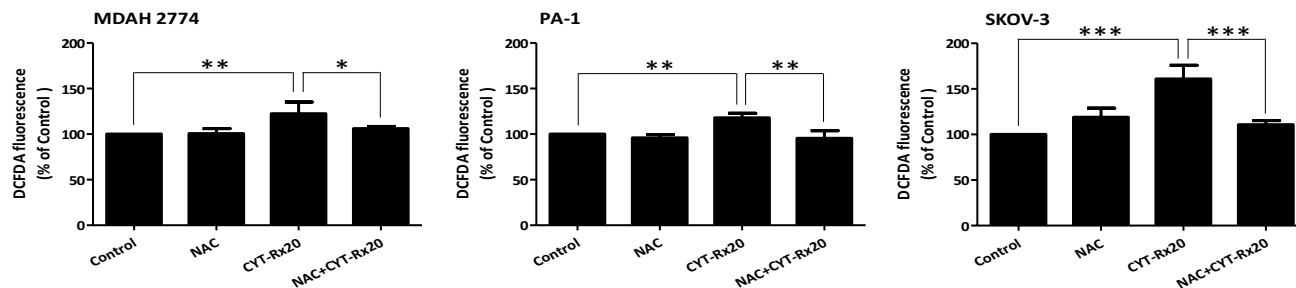
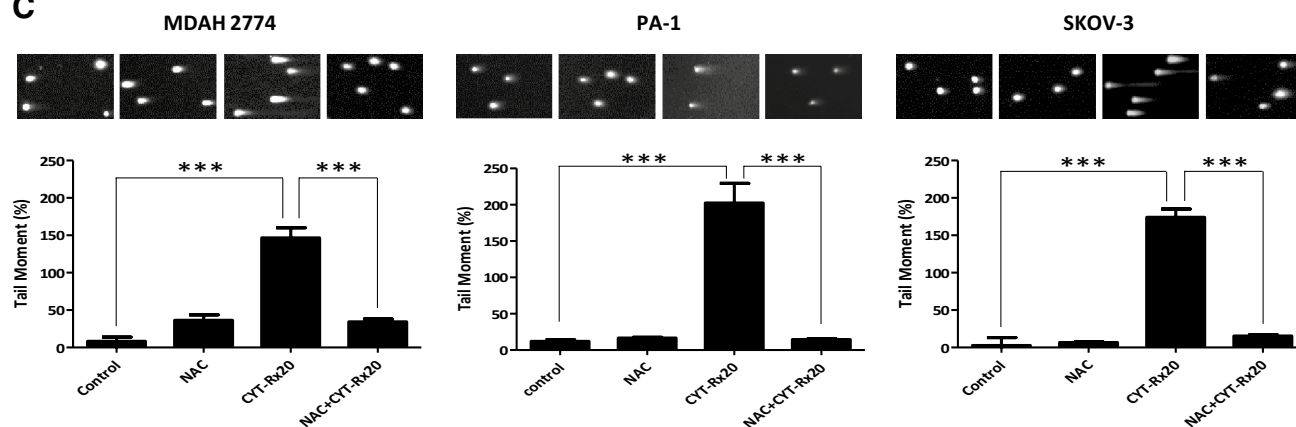
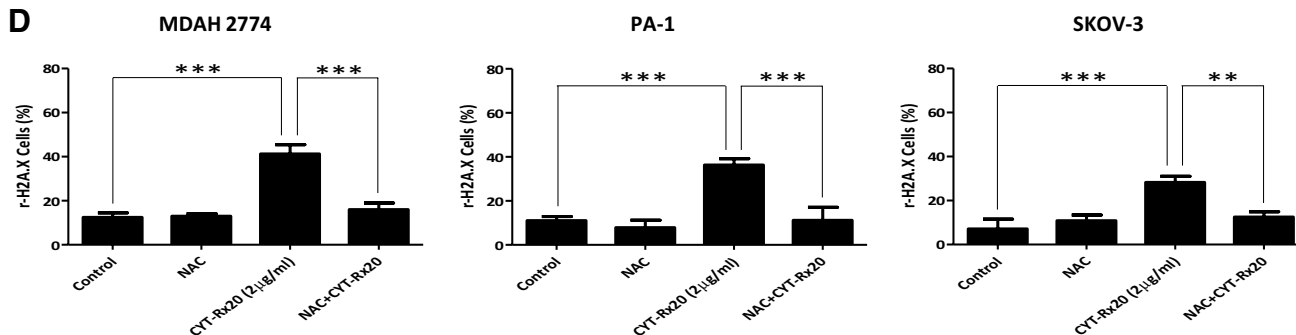
A**CYT-Rx20****B****C****D**

Fig. 1 Effect of ROS inhibitor NAC on CYT-Rx20-induced ROS generation and DNA damage in ovarian cancer cells. **a** Chemical structure of CYT-Rx20. **b** Cells were treated with NAC (5 mM) and/or CYT-Rx20 (2 µg/ml) for 1 h, followed by detection of ROS using H2DCFDA by flow cytometry. **c** Cells were pretreated with NAC (5 mM) for 1 h, followed by CYT-Rx20 (2 µg/mL) treatment for 24 h prior to determination of DNA damage by neutral comet

assay. **d** Cells were pretreated with NAC (10 mM) for 1 h, followed by CYT-Rx20 (2 µg/ml) treatment for 24 h, and the effect of CYT-Rx20 on induction of γ-H2AX focus formation on ovarian cancer cells was evaluated by fluorescence microscope (original magnification ×1000). The data were presented as mean ± SD or mean ± SEM. **P* < 0.05, ***P* < 0.01, ****P* < 0.001 compared with the indicated group by one-way ANOVA

Table 1 Cytotoxicity of CYT-Rx20, CYT-Rx21, CYT-Rx22, CYT-Rx44, CYT-Rx45, CYT-Rx46, and CYT-Rx47 on SKOV3 human ovarian cancer cells

Cell lines	IC ₅₀ (μg/ml) ^a						
	CYT-Rx20	CYT-Rx21	CYT-Rx22	CYT-Rx44	CYT-Rx45	CYT-Rx46	CYT-Rx47
SKOV3	1.39 ± 0.01	>6	1.42 ± 0.02	>4	3.12 ± 0.12	>6	4.10 ± 0.06

Cells were treated with various concentrations of CYT-Rx compounds for 24 h before assessment with XTT assay

^a Data were presented as mean ± SD from three independent experiments

Table 2 Cytotoxicity of CYT-Rx20 and cisplatin on human ovarian cancer cell lines

	IC ₅₀ (μg/ml) ^a	
	CYT-Rx20 (μg/ml)	Cisplatin (μg/ml)
Ovarian cell lines		
MDAH 2774	2.41 ± 0.16	4.78 ± 0.38
PA-1	2.35 ± 0.16	1.94 ± 0.03
SKOV-3	2.48 ± 0.08	6.60 ± 0.96

Cells were treated with various concentrations of CYT-Rx20 or cisplatin for 24 h before assessment with XTT assay

^a Data were presented as mean ± SD from three independent experiments

CYT-Rx20 inhibited ovarian cancer cell viability through induction of apoptosis

CYT-Rx20-induced cell death, determined by XTT colorimetric assay, was dose-dependent and was rescued in the presence of NAC (Suppl. Figure 3; Fig. 2a). It was also rescued by two other thiol antioxidants, glutathione (GSH) and 2-mercaptoethanol (2-ME) (Fig. 2b). CYT-Rx20 treatment decreased the levels of pro-caspase-3 and -9 and PARP, while it increased the levels of cleaved caspase-3 and -9, cleaved PARP, and γ-H2AX (Fig. 2c) in ovarian cancer cells. In this study, the CYT-Rx20-induced apoptotic cell death was further confirmed by annexin V/PI staining and the result showed CYT-Rx20 treatment increased the number of annexin V-positive cells at 24 and 48 h after treatment (Fig. 2d).

Effect of CYT-Rx20 on ovarian cancer cell migration in vitro

Anoikis is a type of programmed cell death that may happen when cells are detached from the extracellular matrix [20]. After CYT-Rx20 treatment, anoikis in ovarian cancer cells was increased in a dose-dependent manner (Fig. 3a). Furthermore, migration of ovarian cancer cells after CYT-Rx20 treatment for 24 h and measured by a modified Boyden chamber assay showed a reduction compared with

that of untreated control (Fig. 3b). A crucial event in cancer cell migration is epithelial–mesenchymal conversion, and the expression of epithelial to mesenchymal transition (EMT) markers is required for the early steps of metastasis [21, 22]. In this study, the protein levels of epithelial marker E-cadherin and mesenchymal markers Vimentin and Twist in ovarian cancer cells were determined by immunoblotting analysis. The expression of E-cadherin was increased in ovarian cancer cells when treated with the indicated concentrations of CYT-Rx20, compared with the control (Fig. 3c). In contrast, the expression of Vimentin and Twist in ovarian cancer cells was decreased after CYT-Rx20 treatment, compared with control cells (Fig. 3c).

CYT-Rx20 inhibited xenografted tumor growth in mice

The inhibitory effect of CYT-Rx20 on anchorage-independent growth of ovarian cancer cells was evaluated by soft agar assay (Fig. 4). CYT-Rx20 significantly inhibited the anchorage-independent growth of ovarian cancer cells (Fig. 4a). To further explore the anticancer activity of CYT-Rx20 in vivo, a nude mice xenograft tumor growth model was employed. As shown in Fig. 4b, c, CYT-Rx20 significantly suppressed xenografted tumor growth in ovarian cancer cells. After CYT-Rx20 treatment for 6 weeks, the average tumor volumes for the control and CYT-Rx20-treated (10.0 μg/g body weight) groups were 126.54 ± 54.87 and 67.13 ± 11.23 mm³, respectively (Fig. 4b), while the average tumor weights at kill were 0.10 ± 0.04 and 0.06 ± 0.03 g, respectively (Fig. 4c). The in vivo effect of CYT-Rx20 on the expression of DNA damage marker γH2AX and mesenchymal marker Vimentin in ovarian tumor xenografts in mice was examined by IHC staining. The expression of γH2AX (Fig. 4d) in xenografted tumors was increased in mice treated with CYT-Rx20. In contrast, the expression of Vimentin was decreased in xenografted tumors of mice treated with CYT-Rx20 (Fig. 4e). No significant differences were observed in the body weight (Suppl. Figure 4a), blood biochemical parameters (Suppl. Table 1), or histology of the ovary, heart, liver, lung, and kidney between CYT-Rx20-treated mice and control mice (Suppl. Figure 4b).

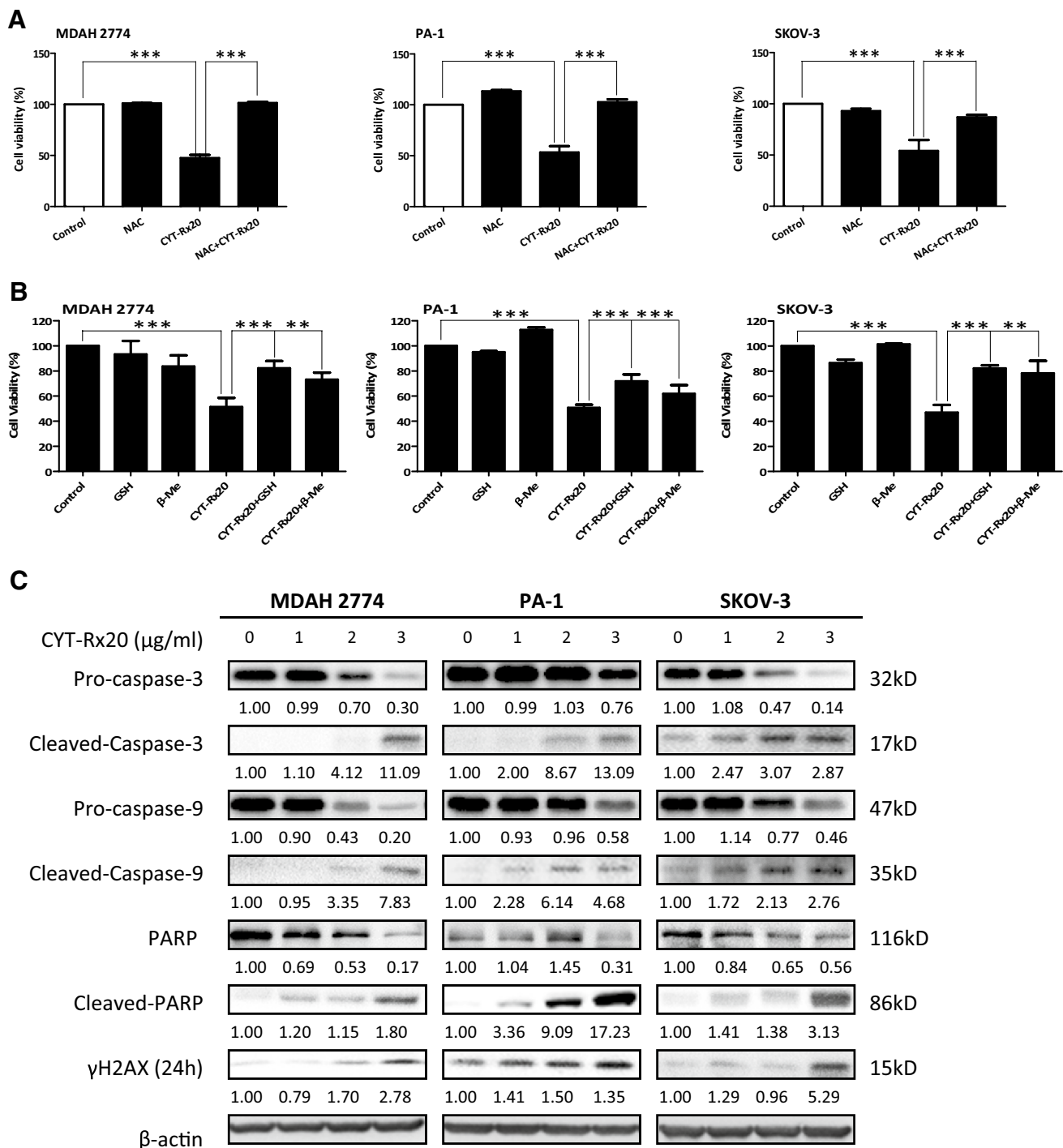


Fig. 2 Cytotoxic effect of CYT-Rx20 on ovarian cancer cells. **a** Cells were pretreated with NAC (10 mM) for 1 h, followed by CYT-Rx20 treatment for 24 h prior to examination of cell viability. **b** Cells were pretreated with glutathione (GSH; 1 mM) or 2-mercaptoethanol (2-ME; 100 μM) for 1 h, followed by CYT-Rx20 (2 μg/mL) treatment for 24 h prior to XTT assay. **c** The expression of apoptosis-related proteins in ovarian cancer cells treated with CYT-Rx20 for

24 h was analyzed by immunoblotting. The expression of β-actin was used as the internal control. The results were representative of three separate experiments. **d** Ovarian cancer cell death after CYT-Rx20 (2 μg/mL) treatment for 24 or 48 h was determined using annexin V/PI staining followed by flow cytometric analysis. The data were presented as mean ± SD. * $P < 0.05$, ** $P < 0.01$, *** $P < 0.001$ compared with the indicated group by one-way ANOVA

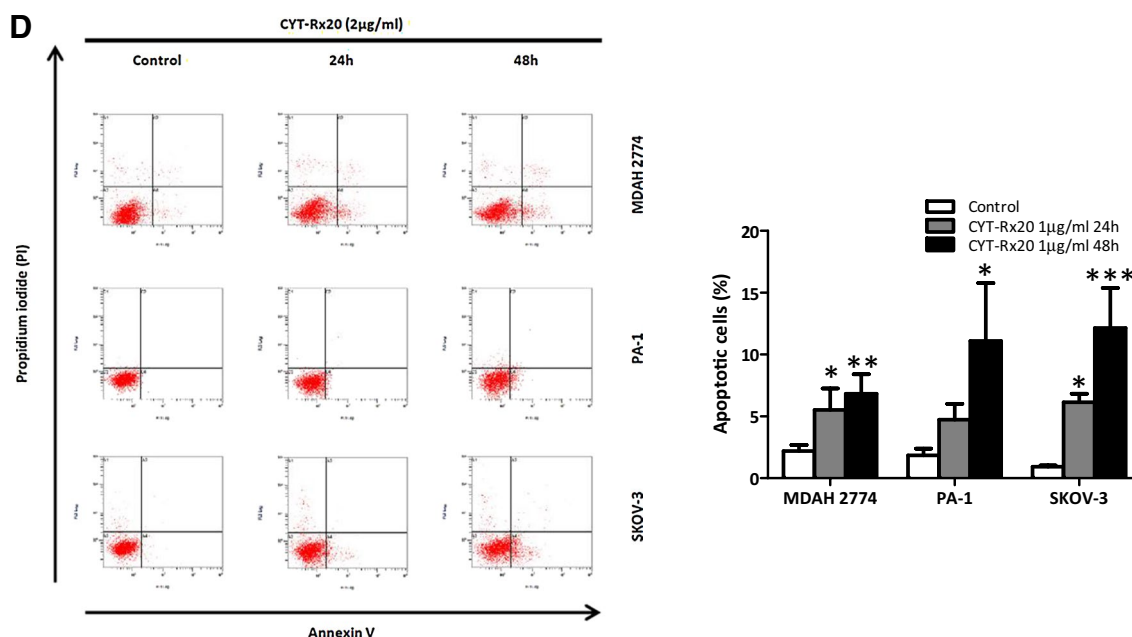


Fig. 2 continued

Discussion

In the current study, we demonstrated for the first time that CYT-Rx20, a synthetic derivative of β -nitrostyrene, significantly reduced cell viability and induced apoptotic cell death in ovarian cancer cells, and it exhibited a higher potency against ovarian cancer cells than the clinically used chemotherapeutic agent CDDP. CYT-Rx20 also decreased ovarian tumor growth in a mouse xenograft model. These results provide in vitro and in vivo evidence for the anti-neoplastic activity of CYT-Rx20 in ovarian cancer.

Reactive oxygen species (ROS) are generated as a normal product of cellular metabolism. Various environmental stresses lead to excessive production of ROS, causing progressive oxidative damage and ultimately cell death. Under environmental stress, ROS are overproduced and then interfere with the stability of mitochondrial membrane potential, leading to an excessive release of mitochondrial ROS followed by cell death [23]. In this study, we provided evidence that CYT-Rx20 treatment induced ROS accumulation and ovarian cancer cell death. Furthermore, ROS can be generated through uncontrolled electron delivery or deficiency in ROS scavengers such as GSH, a major intracellular antioxidant responsible for maintaining the cellular redox state and protecting cells from oxidative damage [24–26]. Our results showed that the CYT-Rx20-induced cytotoxicity in ovarian cancer cells was significantly attenuated by thiol antioxidants NAC, GSH, and β -mercaptoethanol, suggesting that the anticancer activities of CYT-Rx20 may result from the imbalance of thiol redox status. Similar to

our previous study on breast cancer cells [11], we found that CYT-Rx20 treatment leads to ROS accumulation in ovarian cancer cells. Our previous study showed that CYT-Rx20 promoted breast cancer cell death and autophagy through ROS-mediated MEK/ERK pathway. The activation of autophagy can be significantly reversed by thiol group and partially reversed by ERK inhibitors in breast cancer cells [11]. However, the increase of phospho-ERK was not observed in the present study, which might be due to the cell-type specificity.

The increased ROS accumulation in cells may also induce oxidative damage to DNA, including strand breaks and base and nucleotide modifications [27]. On the other hand, DNA damage also induces ROS generation through the H2AX-Nox1/Rac1 pathway [28]. In this study, we monitored DSBs by two approaches, γ -H2AX foci formation assay and neutral comet assay [29, 30]. Our results from both assays provided evidence of DSB induction in a dose-dependent manner after CYT-Rx20 treatment. We also found that CYT-Rx20-mediated γ -H2AX foci formation and DSB were inhibited by NAC in all the ovarian cancer cell lines we tested, suggesting that DNA damage is involved in CYT-Rx20-induced cell death.

Our findings showed that apoptosis is involved in CYT-Rx20-induced cell growth inhibition in ovarian cancer cells, evident by the increased number of annexin V-positive cells. It is well known that members of the caspase family mediated apoptotic programmed cell death in various cancer cell types including ovarian cancer [31]. Caspase-9 is activated very early in the apoptotic cascade by

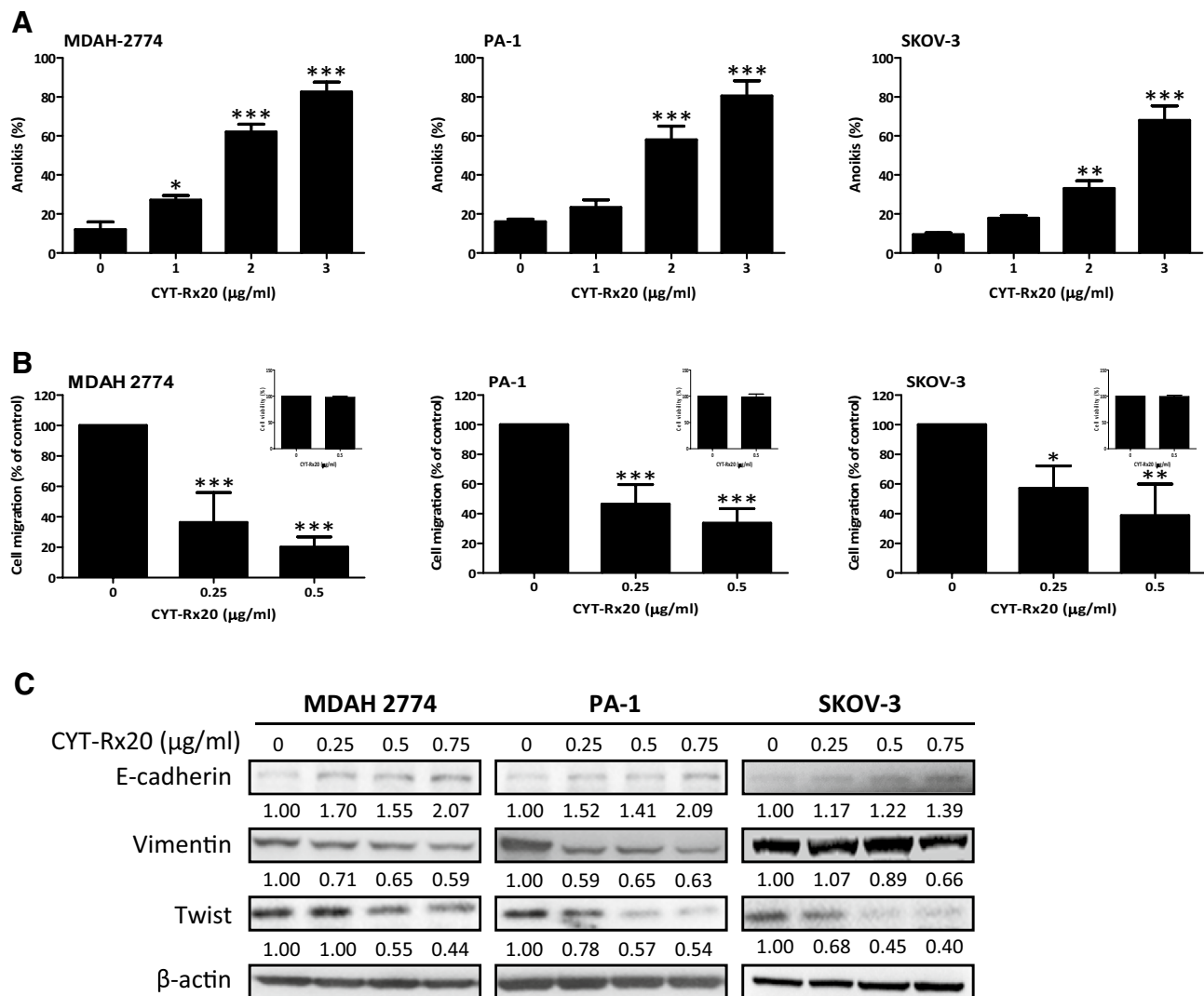


Fig. 3 Effect of CYT-Rx20 on ovarian cancer cell migration. **a** Ovarian cancer cells were treated with CYT-Rx20 for 24 h and then collected after 24 h of anoikis induction for evaluation of cell death rate, determined by trypan blue staining using hemocytometer. **b** Ovarian cancer cells were treated with CYT-Rx20 for 24 h and the migration efficiencies were determined using a modified Boyden chamber assay. **c** Protein expression of epithelial to mesenchymal transition

(EMT) markers was analyzed by immunoblotting after three ovarian cancer cell lines were treated with the indicated concentrations of CYT-Rx20 for 24 h. The intensity of the protein band after normalization to the internal control β -actin was calculated as the fold of controls and then depicted as histograms. The data were presented as mean \pm SD. * P < 0.05, ** P < 0.01, *** P < 0.001 compared with the indicated group by one-way ANOVA

cytochrome c, which is released from the mitochondria in response to apoptotic stimuli, followed by the activation of downstream caspases including caspase-3 and the cleavage of PARP, a hallmark of apoptosis [32]. In this study, we showed that CYT-Rx20 treatment of ovarian cancer cells resulted in the activation of caspase-9, caspase-3, and the cleavage of PARP. These results suggested that CYT-Rx20 exerted strong anticancer activity on ovarian cancer by inducing apoptosis.

CYT-Rx20 treatment of ovarian cancer cells promoted anoikis, a form of cell death induced upon cell

detachment from the extracellular matrix [20]. Recent evidence has suggested that the process of epithelial to mesenchymal transition (EMT) may play a role in the development of chemoresistance [33]. The main characteristics of EMT are the up-regulation of extracellular matrix components, loss of intercellular cohesion, increased ability of cellular migration and invasion, and increased resistance to apoptosis [34]. In agreement with these findings, our study demonstrated that CYT-Rx20 treatment suppressed the migration of ovarian tumor cells through activation of epithelial marker (E-cadherin)

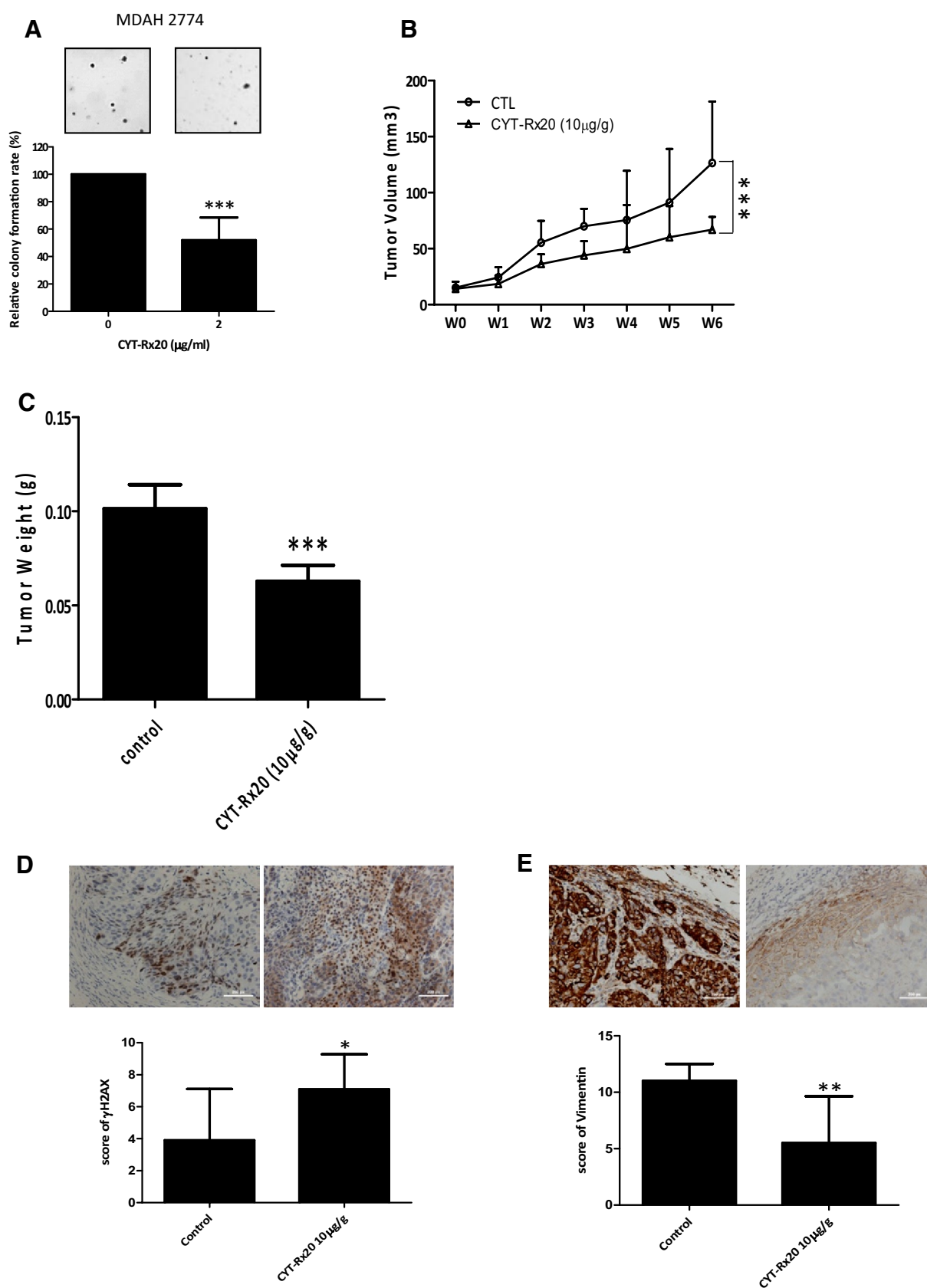


Fig. 4 Effect of CYT-Rx20 on ovarian cancer tumorigenesis in vitro and in vivo. **a** MDAH 2774 cells were treated with CYT-Rx20 (2 µg/mL) for 24 h, followed by evaluation of anchorage-independent colony formation using soft agar assay as described in “Materials and methods”. **b** Female nude mice subcutaneously xenografted with MDAH 2774 cells were intraperitoneally treated with 0.1% DMSO in normal saline (control) or 10 µg/g body weight of CYT-Rx20 three times per week ($n = 10$ for each group). Tumor volume was measured every three days according to the formula $(\text{width}^2 \times \text{length})/2$. **c** Tumor weight was measured when mice were killed at the end of study. **d** The expression of γ H2AX and **e** Vimentin in xenografted tumor tissues was analyzed by immunohistochemistry. The representative photographs were shown with $\times 200$ magnification. Bar represents 200 µm. The data were presented as mean \pm SD. * $P < 0.05$, ** $P < 0.01$, *** $P < 0.001$, compared with the indicated group by one-way ANOVA

and inactivation of mesenchymal markers (Vimentin and Twist). These results suggested that CYT-Rx20 inhibited not only the proliferation but also the migratory capabilities of cancer cells.

The anticancer activity of CYT-Rx20 was also evaluated in vivo. We found that CYT-Rx20 suppressed xenografted ovarian tumor growth associated with the increased expression of γ -H2AX and decreased expression of Vimentin in tumor tissues. There were no obvious abnormal histological changes in the examined organs of nude mice (including ovary), and no impairment in hematopoiesis, renal or liver function (Suppl. Table 1), rendering CYT-Rx20 a potential anti-ovarian cancer agent with low toxicity.

Taken together, the present study demonstrated that the synthetic β -nitrostyrene derivative CYT-Rx20 induced apoptosis in ovarian cancer cells through a ROS induction pathway. Our findings indicate that CYT-Rx20 may be developed as a potential chemotherapeutic agent for ovarian cancer. Further pre-clinical and clinical studies are required to confirm its therapeutic potential for ovarian cancer treatment.

Acknowledgements This study was supported by Grants from the Ministry of Health and Welfare (MOHW105-TDU-B-212-134007 and MOHW105-TDU-B-212-112016, Health and welfare surcharge of tobacco products) of Taiwan and National Health Research Institutes (NHRI-EX104-10212BI).

Compliance with ethical standards

Conflict of interest Yen-Yun Wang, Yuk-Kwan Chen, Stephen Chu-Sung Hu, Ya-Ling Hsu, Chun-Hao Tsai, Tsung-Chen Chi, Wan-Ling Huang, Pei-Wen Hsieh, and Shyng-Shiou F. Yuan have declared no conflict of interest.

Ethical approval The animal studies were approved by the Institutional Animal Care and Use Committee (IACUC No. 102009) of Kaohsiung Medical University, Taiwan. Animal experiments were approved by the Laboratory Animal Ethics Committee of Kaohsiung Medical University.

References

1. Siegel R, Naishadham D, Jemal A (2013) Cancer statistics. *CA Cancer J Clin* 63(1):11–30. doi:10.3322/caac.21166
2. Sherman-Baust CA, Becker KG, Wood Iii WH, Zhang Y, Morin PJ (2011) Gene expression and pathway analysis of ovarian cancer cells selected for resistance to cisplatin, paclitaxel, or doxorubicin. *J Ovarian Res* 4(1):21. doi:10.1186/1757-2215-4-21
3. Romero I, Bast RC Jr (2012) Minireview: human ovarian cancer: biology, current management, and paths to personalizing therapy. *Endocrinology* 153(4):1593–1602. doi:10.1210/en.2011-2123
4. Park J, Pei D (2004) Trans-beta-nitrostyrene derivatives as slow-binding inhibitors of protein tyrosine phosphatases. *Biochemistry* 43(47):15014–15021. doi:10.1021/bi0486233
5. Chen IH, Chang FR, Wu YC, Kung PH, Wu CC (2015) 3,4-Methylenedioxy-beta-nitrostyrene inhibits adhesion and migration of human triple-negative breast cancer cells by suppressing beta1 integrin function and surface protein disulfide isomerase. *Biochimie* 110:81–92. doi:10.1016/j.biochi.2015.01.006
6. Rahmani-Nezhad S, Safavi M, Pordeli M, Ardestani SK, Khosravani L, Pourshojaei Y, Mahdavi M, Emami S, Foroumadi A, Shafiee A (2014) Synthesis, in vitro cytotoxicity and apoptosis inducing study of 2-aryl-3-nitro-2H-chromene derivatives as potent anti-breast cancer agents. *Eur J Med Chem* 86:562–569. doi:10.1016/j.ejmech.2014.09.017
7. Hsieh PW, Chang YT, Chuang WY, Shih HC, Chiang SZ, Wu CC (2010) The synthesis and biologic evaluation of anti-platelet and cytotoxic beta-nitrostyrenes. *Bioorg Med Chem* 18(21):7621–7627. doi:10.1016/j.bmc.2010.08.039
8. He Y, Varadarajan S, Munoz-Planillo R, Burberry A, Nakamura Y, Nunez G (2014) 3,4-Methylenedioxy-beta-nitrostyrene inhibits NLRP3 inflammasome activation by blocking assembly of the inflammasome. *J Biol Chem* 289(2):1142–1150. doi:10.1074/jbc.M113.515080
9. Carter KC, Fannon YS, Daeid NN, Robson DC, Waddell R (2002) The effect of nitrostyrene on cell proliferation and macrophage immune responses. *Immunopharmacol Immunotoxicol* 24(2):187–197. doi:10.1081/iph-120003749
10. Zeng Z, Sun Z, Huang M, Zhang W, Liu J, Chen L, Chen F, Zhou Y, Lin J, Huang F, Xu L, Zhuang Z, Guo S, Alitongbieke G, Xie G, Xu Y, Lin B, Cao X, Su Y, Zhang XK, Zhou H (2015) Nitrostyrene derivatives act as RXRalpha ligands to inhibit TNFalpha activation of NF-kappaB. *Cancer Res* 75(10):2049–2060. doi:10.1158/0008-5472.can-14-2435
11. Hung AC, Tsai CH, Hou MF, Chang WL, Wang CH, Lee YC, Ko A, Hu SC, Chang FR, Hsieh PW, Yuan SS (2016) The synthetic beta-nitrostyrene derivative CYT-Rx20 induces breast cancer cell death and autophagy via ROS-mediated MEK/ERK pathway. *Cancer Lett* 371(2):251–261. doi:10.1016/j.canlet.2015.11.035
12. Wang WY, Hsieh PW, Wu YC, Wu CC (2007) Synthesis and pharmacological evaluation of novel beta-nitrostyrene derivatives as tyrosine kinase inhibitors with potent antiplatelet activity. *Biochem Pharmacol* 74(4):601–611. doi:10.1016/j.bcp.2007.06.001
13. Chen HM, Wu YC, Chia YC, Chang FR, Hsu HK, Hsieh YC, Chen CC, Yuan SS (2009) Gallic acid, a major component of Toona sinensis leaf extracts, contains a ROS-mediated anticancer activity in human prostate cancer cells. *Cancer Lett* 286(2):161–171. doi:10.1016/j.canlet.2009.05.040
14. Yuan SS, Hou MF, Hsieh YC, Huang CY, Lee YC, Chen YJ, Lo S (2012) Role of MRE11 in cell proliferation, tumor invasion, and DNA repair in breast cancer. *J Natl Cancer Inst* 104(19):1485–1502. doi:10.1093/jnci/djs355
15. Krajewska M, Krajewski S, Epstein JI, Shabaik A, Sauvageot J, Song K, Kitada S, Reed JC (1996) Immunohistochemical

- analysis of bcl-2, bax, bcl-X, and mcl-1 expression in prostate cancers. *Am J Pathol* 148(5):1567–1576
16. Alfadda AA, Sallam RM (2012) Reactive oxygen species in health and disease. *J Biomed Biotechnol* 2012:936486. doi:[10.1155/2012/936486](https://doi.org/10.1155/2012/936486)
 17. Costa A, Scholer-Dahirel A, Mechta-Grigoriou F (2014) The role of reactive oxygen species and metabolism on cancer cells and their microenvironment. *Semin Cancer Biol* 25:23–32. doi:[10.1016/j.semcancer.2013.12.007](https://doi.org/10.1016/j.semcancer.2013.12.007)
 18. Reczek CR, Chandel NS (2015) ROS-dependent signal transduction. *Curr Opin Cell Biol* 33:8–13. doi:[10.1016/j.ceb.2014.09.010](https://doi.org/10.1016/j.ceb.2014.09.010)
 19. Kuo LJ, Yang LX (2008) Gamma-H2AX-a novel biomarker for DNA double-strand breaks. *In vivo* 22(3):305–309
 20. Paoli P, Giannoni E, Chiarugi P (2013) Anoikis molecular pathways and its role in cancer progression. *Biochim Biophys Acta* 12:3481–3498. doi:[10.1016/j.bbamcr.2013.06.026](https://doi.org/10.1016/j.bbamcr.2013.06.026) (pii:S0167-4889(13)00249-8)
 21. Scheel C, Weinberg RA (2012) Cancer stem cells and epithelial-mesenchymal transition: concepts and molecular links. *Semin Cancer Biol* 22(5–6):396–403. doi:[10.1016/j.semcancer.2012.04.001](https://doi.org/10.1016/j.semcancer.2012.04.001)
 22. Tsai JH, Yang J (2013) Epithelial-mesenchymal plasticity in carcinoma metastasis. *Genes Dev* 27(20):2192–2206. doi:[10.1101/gad.225334.113](https://doi.org/10.1101/gad.225334.113)
 23. Dickinson BC, Chang CJ (2011) Chemistry and biology of reactive oxygen species in signaling or stress responses. *Nat Chem Biol* 7(8):504–511. doi:[10.1038/nchembio.607](https://doi.org/10.1038/nchembio.607)
 24. Pan ST, Qin Y, Zhou ZW, He ZX, Zhang X, Yang T, Yang YX, Wang D, Qiu JX, Zhou SF (2015) Plumbagin induces G2/M arrest, apoptosis, and autophagy via p38 MAPK- and PI3 K/Akt/mTOR-mediated pathways in human tongue squamous cell carcinoma cells. *Drug Des Devel Ther* 9:1601–1626. doi:[10.2147/dddt.s76057](https://doi.org/10.2147/dddt.s76057)
 25. Armstrong JS, Steinauer KK, Hornung B, Irish JM, Lecane P, Birrell GW, Peehl DM, Knox SJ (2002) Role of glutathione depletion and reactive oxygen species generation in apoptotic signaling in a human B lymphoma cell line. *Cell Death Differ* 9(3):252–263. doi:[10.1038/sj.cdd.4400959](https://doi.org/10.1038/sj.cdd.4400959)
 26. Rahman I, Biswas SK, Jimenez LA, Torres M, Forman HJ (2005) Glutathione, stress responses, and redox signaling in lung inflammation. *Antioxid Redox Signal* 7(1–2):42–59. doi:[10.1089/ars.2005.7.42](https://doi.org/10.1089/ars.2005.7.42)
 27. Burney S, Niles JC, Dedon PC, Tannenbaum SR (1999) DNA damage in deoxynucleosides and oligonucleotides treated with peroxynitrite. *Chem Res Toxicol* 12(6):513–520. doi:[10.1021/tx980254m](https://doi.org/10.1021/tx980254m)
 28. Kang MA, So EY, Simons AL, Spitz DR, Ouchi T (2012) DNA damage induces reactive oxygen species generation through the H2AX-Nox1/Rac1 pathway. *Cell death Dis* 3:e249. doi:[10.1038/cddis.2011.134](https://doi.org/10.1038/cddis.2011.134)
 29. Bekker-Jensen S, Mailand N (2010) Assembly and function of DNA double-strand break repair foci in mammalian cells. *DNA Repair* 9(12):1219–1228. doi:[10.1016/j.dnarep.2010.09.010](https://doi.org/10.1016/j.dnarep.2010.09.010)
 30. Olive PL, Banath JP (2006) The comet assay: a method to measure DNA damage in individual cells. *Nat Protoc* 1(1):23–29. doi:[10.1038/nprot.2006.5](https://doi.org/10.1038/nprot.2006.5)
 31. Yang X, Zheng F, Xing H, Gao Q, Wei W, Lu Y, Wang S, Zhou J, Hu W, Ma D (2004) Resistance to chemotherapy-induced apoptosis via decreased caspase-3 activity and overexpression of antiapoptotic proteins in ovarian cancer. *J Cancer Res Clin Oncol* 130(7):423–428. doi:[10.1007/s00432-004-0556-9](https://doi.org/10.1007/s00432-004-0556-9)
 32. Nicholson DW, Thornberry NA (1997) Caspases: killer proteases. *Trends Biochem Sci* 22(8):299–306
 33. Voulgari A, Pintzas A (2009) Epithelial-mesenchymal transition in cancer metastasis: mechanisms, markers and strategies to overcome drug resistance in the clinic. *Biochim Biophys Acta* 1796(2):75–90. doi:[10.1016/j.bbcan.2009.03.002](https://doi.org/10.1016/j.bbcan.2009.03.002)
 34. Haslehurst AM, Koti M, Dharsee M, Nuin P, Evans K, Geraci J, Childs T, Chen J, Li J, Weberpals J, Davey S, Squire J, Park PC, Feilottter H (2012) EMT transcription factors snail and slug directly contribute to cisplatin resistance in ovarian cancer. *BMC Cancer* 12:91. doi:[10.1186/1471-2407-12-91](https://doi.org/10.1186/1471-2407-12-91)